GREEN SYNTHESIS OF SILVER NANOPARTICLES USING *Parmelia sulcata Taylor* EXTRACT AND ITS APPLICATION IN COLORIMETRIC SENSING OF ORGANOPHOSPHORUS PESTICIDE

A DISSERTATION

SUBMITTED FOR THE PARTIAL FULLFILLMENT OF THE REQUIREMENTS FOR THE MASTERS OF SCIENCE DEGREE IN CHEMISTRY

By

Aarati Ray

Exam Roll No.: CHE 701/073

Reg. No.:5-2-0038-0033-2012

CENTRAL DEPARTMENT OF CHEMISTRY

INSTITUTE OF SCIENCE AND TECHNOLOGY

TRIBHUVAN UNIVERSITY

KIRTIPUR, KATHMANDU

NEPAL

JANUARY, 2021

BOARD OF EXAMINER AND CERTIFICATE OF APPROVAL

This dissertation entitled "**Green synthesis of silver nanoparticles using *Parmelia sulcata Taylor* extract and its application in colorimetric sensing of organophosphorus pesticide**" by Ms. *Aarati Ray*, under the supervision of *Dr. Achyut Adhikari (Assoc. Prof.), Central Department of Chemistry,* Tribhuvan University, Nepal, is hereby submitted for the partial fulfillment of the Master of Science (M. Sc.) degree in Chemistry. This dissertation has been awarded for a degree.

……

Supervisor

Dr. Achyut Adhikari

Associate Professor

Central Department of Chemistry

Tribhuvan University, Kirtipur

Kathmandu, Nepal

……

Head of the Department

Prof. Dr. Ram Chandra Basnyat

Central Department of Chemistry

Tribhuvan University, Kirtipur

Kathmandu, Nepal

……

External Examiner

Dr. Surendra Kumar Gautam

Associate Professor

Trichandra Multiple Campus

Ghantaghar, Kathmandu

Nepal

……..

Internal Examiner

Dr. Bhanu Bhakta Neupane

Assistant Professor

Central Department of Chemistry

Tribhuvan University, Kirtipur

Kathmandu, Nepal

Date: ……

RECOMMENDATION LETTER

This is to certify that the dissertation work entitled "**Green synthesis of silver nanoparticles using *Parmelia sulcata Taylor* extract and its application in colorimetric sensing of organophosphorus pesticide**" has been carried out by **Ms. Aarati Ray** as partial fulfillment for the requirements of M. Sc. degree in Chemistry under my supervision. To the best of my knowledge, this dissertation work has not been submitted for any other degree in this institute.

……..

Supervisor

Dr. Achyut Adhikari

Associate Professor

Central Department of Chemistry

Tribhuvan University, Kirtipur

Kathmandu, Nepal

Date: ……

DECLARATION

I, "*Aarati Ray*", hereby declare that the work presented herein is genuine work done originally by me and has not been published or submitted elsewhere for the requirement of a degree program. Any literature, data or works done by others and cited in this dissertation has been given due acknowledgement and listed in the reference section.

…….

Aarati Ray

Date: ……

ACKNOWLEDGEMENTS

This thesis becomes a reality with the kind support and help of many individuals, I would like to extend my sincere thanks to all of them.

Foremost, I would like to express my profound gratitude to my supervisor **Dr. Achyut Adhikari (Assoc. Prof.)** for his continuous guidance, suggestion and encouragement throughout my work. Without his supervision this research work would be incomplete.

I would like to thank **Prof. Dr. Ram Chandra Basnyat**, Head of Central Department of Chemistry (HOD), Tribhuvan University, for providing me an opportunity to conduct this dissertation. I would also like to express my sincere gratitude to all the respected professors of CDC for their valuable suggestions and inspiration. I am also thankful to all the administrative and laboratory staffs of CDC for their worthful assistance during my laboratory work at CDC.

I am grateful to **University Grants Commission** (UGC) for providing fund to carry out my thesis work considering award no.: **MRS-75/76, S & T-13**. I owe my deep gratitude to **Mr. Subhash Khatri**, **Mr. Amrit K.C.**, Research Officers, National Herbarium & Plant Laboratories (NHPL), Godawari, who helped me to identify the plant species. I am also thankful to **Mr. Basanta Giri** and **Mr. Shishir Pandey**, Kathmandu Institute of Applied Sciences (KIAS) for making available malathion and sharing knowledge about pesticides.

I am equally grateful to **Dr. Suresh Kumar Dhungel**, Nepal Academy of Science and Technology (NAST), for his assistance with XRD. I would also like to express my special thanks to **Dr. Gobinda Gyawali**, Sun Moon University for SEM and EDX results.

I would like to express my special thanks to **Ms. Rasna Maharjan, Mr. Maheshwar Mahato** and **Mr. Pradip Chaudhary** for helping me throughout and my brother-in-law **Mr. Kundan Chaudhari** for helping in lichen collection. My thanks and appreciations also goes to my family especially my dad **Mr. Bhuneshwar Prasad Ray** and my mom **Mrs. Sona Devi Ray**, friends and people who have willingly helped me out with their abilities.

Thank you.

LIST OF SYMBOLS AND ABBREVIATIONS

ACh	Acetylcholine
AChE	Acetyl cholinesterase
AFM	Atomic force microscopy
Ag NPs	Silver nanoparticles
EDX	Energy dispersive X-ray
HRTEM	High-resolution transmission electron microscopy
OPPs	Organophosphorus pesticides
PELs	Permissible exposure limits
rpm	Revolution per minute
SEM	Scanning electron microscopy
SERS	Surface-enhanced raman spectroscopy
SPR	Surface plasmon resonance
STM	Scanning tunneling microscopy
TEM	Transmission electron microscopy
UV-vis	Ultraviolet-visible
XRD	X-ray diffraction

ABSTRACT

A cost effective and environment friendly synthesis of silver nanoparticles using aqueous extract of *Parmelia sulcata* has been done. Formation of silver nanoparticles was confirmed by UV-vis spectra as well as color change. XRD study confirmed that the resultant particles are silver nanoparticles having FCC structure with average crystalline size as 7.46 nm. Formed silver nanoparticles were modified by L-cysteine solution. Characterization of L-cys-Ag NPs was done by UV-visible spectrophotometer measuring optical absorbance which increased from 0.1278 to 0.1581. Organophosphorus pesticide namely malathion was detected by mixing it with modified silver nanoparticles. NaCl stimulated color change from brownish yellow to light yellow depending on malathion concentration of 100 ppm, 10 ppm, 1 ppm, 0.1 ppm and 0.01 ppm. With the decrease in malathion concentration, the absorbance at 430 nm gradually increased. Thus this colorimetric sensor allowed a direct quantitative check for the detection of malathion.

Keywords: Nanoparticles, *Parmelia sulcata Taylor*, Organophosphorus pesticide, L-cysteine

TABLE OF CONTENTS

LIST OF FIGURES

LIST OF TABLES

CHAPTER I

INTRODUCTION

1.1 General Introduction

Nanotechnology is the science and engineering involved in the design, synthesis, characterization, and application of materials and devices whose smallest functional organization in at least one dimension is on the nanometer scale or one billionth of a meter.

1.2 Historical Background

Nanotechnology is the burning term these days for its wide variety of applications in each and every sector. The synthesis of the nanoparticles, however, is a fairly established field as particles of submicron or nanosized dimensions have been synthesized for centuries. The first example of considerable recognition is the Roman Lycurgus Cup, a bronze cup lined with colored glass that dates to the fourth century AD.[1] The glass scatters a dull green light and transmits red light. According to a study commissioned by the British Museum, which currently displays the cup, the glass contains 70 nm particles that are an alloy of silver (70%) and gold (30%). However, Michael Faraday in 1857 conducted the first notable scientific study of the optical properties of metal nanoparticles, colloidal suspensions, and ultrathin metal films by reducing an aqueous solution of chloroauric acid with phosphorus in the presence of carbon disulfide (CS_2) to prepare gold colloids and obtained "ruby fluids" of dispersed gold particles.[2]

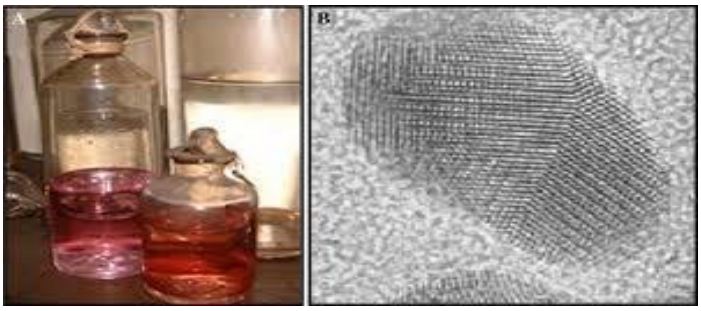

Figure 1.1 Michael Faraday's colloidal gold, suspension reproduced by "Courtesy of the Royal Institution of Great Britain" and HRTEM micrograph of the single gold nanoparticle

The first lecture regarding the application for nanoscale materials was given by Physics Nobel Laureate Richard Feynman, entitled “There is a plenty of Room at the Bottom” was delivered on 29 December 1959 at the annual American Physical Society meeting on the campus of Caltech. He pointed out that there is a real possibility to design materials atom by atom, as it would not violate any physical laws. In 1974, Norio Taniguchi firstly used the term “nanotechnology” referring to “production technology to get extra high accuracy and ultra-fine dimensions, i.e., the preciseness and fineness on the order of 1 nm (nanometer), 10^{-9} m in length”.[3] But it took more than three decades for the research community to translate Feynman's vision into reality.

1.3 Nanoparticles (NPs)

According to the American Society for Testing and Materials (ASTM) standard definition, nanoparticles are particles with lengths that range from 1 to 100 nm in two or three dimensions. It addresses the extremely minute structures using the prefix “nano”, a Greek word which means “dwarf or miniature”.[4,5] NPs exhibit new or improved properties based on specific characteristics such as size, distribution, and morphology. Bulk and atomic structures are different in their properties and the gap between them is bridged by metal NPs with their unique physicochemical properties, i.e., large surface to volume ratio, surface energy, spatial confinement, high surface area, high reactivity, tunable pore size, and particle morphology. The physicochemical and optoelectronic properties of metallic NPs are strongly dependent on size, size distribution, structure, shape, and chemical-physical environment.

The increase in surface area to volume ratio leads to the increasing dominance of the behavior of atoms on the surface of the particle over that of those in the interior of the particle, thus altering its mechanical, thermal, and catalytic properties. A much lower melting point or sintering temperatures of nanoscale materials compared to bulk ones, make it possible to form bonds between neighboring at a lower temperature due to high energy. Bulk counterparts have usually lower mechanical strength than nanostructured material which involves a reduction of crystal defects. Moreover, Quantum confinement effects bring changes in the electronic structure, i.e., the size effect contributed by quantum mechanics, could be used to alter the reactivity of the nano-crystals. This

quantum confinement of electrons which takes place as the reduction of crystal dimensions leads to the appearance of novel electronic, optical, and magnetic properties of nano-systems that is extremely different from their bulk counterparts.[6,7,8]

1.4 Silver Nanoparticles (Ag NPs)

Nowadays, NPs made from noble metals, particularly Ag, Au, Pd, and Pt are most effectively studied.[9,10] Among all noble metal NPs, silver nanoparticles have fascinated researchers because of their unique physical and chemical properties such as high thermal and electrical conductivity, good chemical stability, and nonlinear optical properties.[11] Since the size, shape, and composition of Ag NPs can have a significant effect on their efficacy, extensive research has gone into synthesizing and characterizing Ag NPs.

1.5 Approaches to Nanotechnology

Synthesis of NPs can be done by two different processes such as "Top to bottom" and "Bottom to up" process.[12]

- Top to bottom approach: Breaking down of bulk material into nanoscale particles using various lithographic techniques, e.g., grinding, milling, etc.
- Bottom to up approach: Self-assembly of atoms into new nuclei which grow into a nanoscale particle

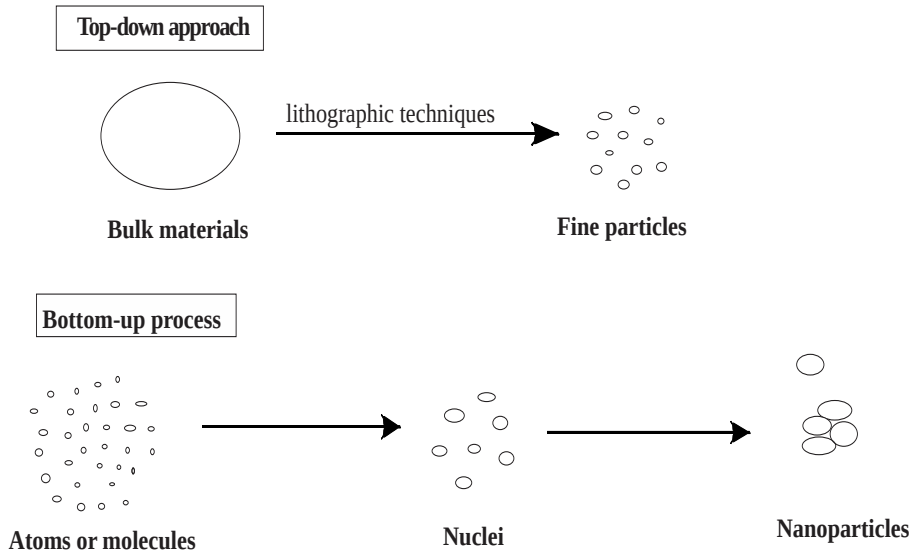

Figure 1.2 Protocols employed for the synthesis of NPs

Development of various physical, chemical, and biological synthesis methods have been done to synthesize NPs of different compositions, sizes, shapes, and controlled polydispersity.

1.5.1 Physical Method

It involves laser ablation and evaporation condensation methods which are expensive due to the continuous consumption of energy while maintaining high temperature and pressure with the requirement of highly sophisticated equipment and a large space.

1.5.2 Chemical Method

It includes aerosol technique, electrochemical or sonochemical deposition, photochemical reduction, laser irradiation technique, and utilizes chemical reductants ($NaBH_4$, ethanol, ethylene glycol, etc.) which generate hazardous by-products.

1.5.3 Green Biological Method

The development of a clean, reliable, eco-friendly process regarding the synthesis of nanomaterials that minimize the use of hazardous procedures through an alternative route is an important aspect of nanotechnology.[13] Biological methods of synthesis have offered a better manipulation and control over crystal growth and their stabilization due to slower kinetics. Along with this, it is environmentally friendly, cost-effective, and easily scaled up for large scale synthesis with no need for high pressure, energy, temperature, and toxic chemical that may have an adverse effect on the medical applications and environment,[14] hence have been proved to be a better approach. Since NPs synthesis has been done using microorganisms, enzymes, and plant or plant extract, we have approached through a plant-mediated one.

1.6 Plant Mediated Synthesis of Ag NPs

Green and rapid NP synthesis methods using plant extracts have drawn attention due to their simplicity, inherent safety, and affordability.[15] Biomolecules contained in plant parts such as water-soluble flavonoids, alkaloids, and several phenolic compounds (phenolic acids, stilbenes, tannins, and lignin) are responsible for the rapid reduction of metal salts along with capping and stabilizing them. These biomolecules affect the morphology of synthesized

NPs.[16,17] It also determines the reduction potential of ions, which in turn determine the amount of NPs accumulated.[18,19]

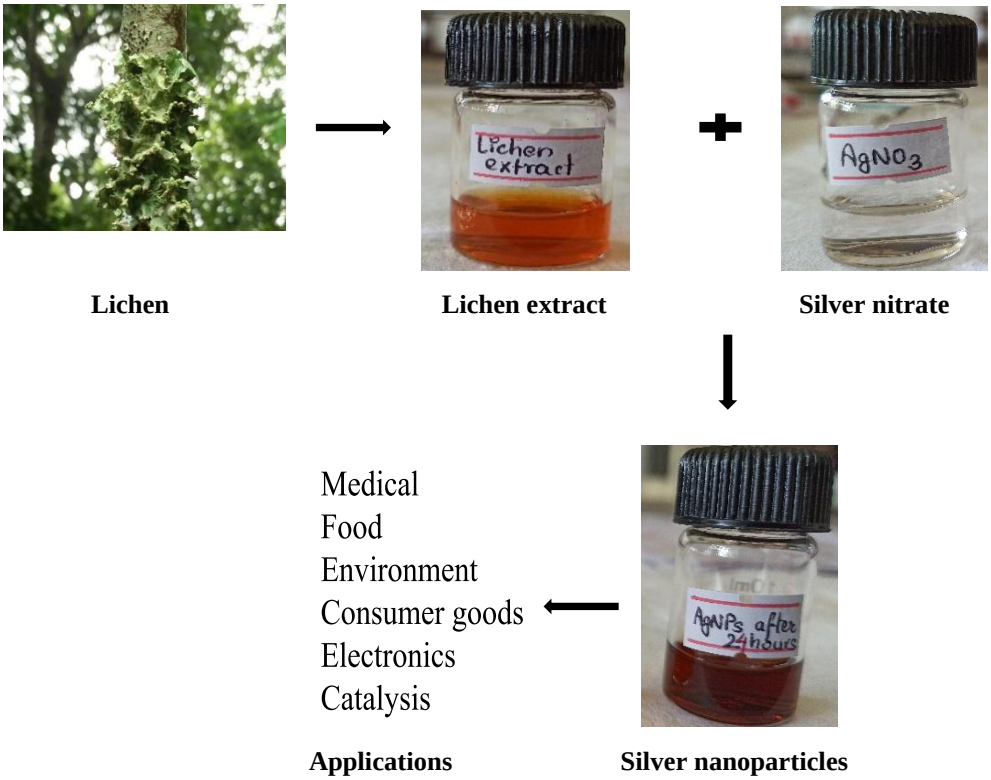

Figure 1.3 Schematic diagram for the synthesis of Ag NPs using plant extract

1.7 Possible Mechanism of Green Synthesis of Ag NPs

Various mechanistic approaches have been proposed by several researchers to understand the hidden pathway involved in the green synthesis of Ag NPs since its exact mechanism is still unknown. The preliminary mechanism involves the accumulation of NPs after the reduction of metal ions which is mediated by some reducing agents i.e., phytochemical components from plants.[17]

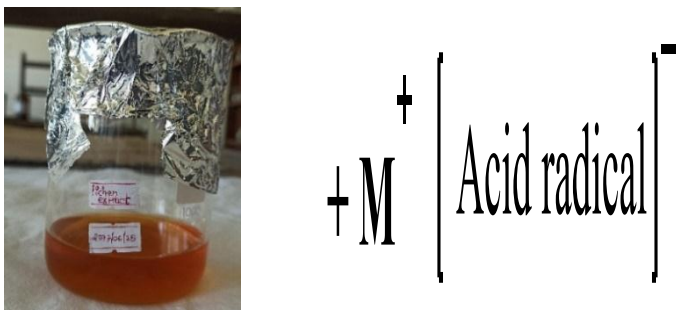

Figure 1.4 A simple schematic of the plant-mediated synthesis process, where metal precursor reacts with a plant extract

In the plant-mediated synthesis of Ag NPs, the ionization of $AgNO_3$ used as a precursor takes place as given below:

$$AgNO_3\ (aq.) = Ag^+\ (aq.) + NO_3^-\ (aq.)$$

The plant molecules which act as electron donor species, are involved in the reduction of Ag ions which act as electron acceptor species involving both oxidation and reduction reactions. Proteins, chlorophyll, and some metabolites present in the plant extracts act as capping and stabilizing agents between donor and acceptor molecules.

The hypothesis behind the core mechanism in the bio-reduction of Ag involves trapping of Ag^+ ions on the protein surface due to electrostatic interactions between the silver ions and proteins in plant material extract. Ag^+ ions are reduced by proteins, leading to their secondary structure change and silver nuclei are formed. These formed silver nuclei successively grow by the further reduction of Ag^+ ions and their build-up at the nuclei leading to the formation of Ag NPs.[16]

Stabilization of Ag NPs is necessary to prevent them from coagulation after their formation. Van der Wall force causes the coagulation therefore; there must be a repulsive force to overcome it to stabilize NPs in a dispersing medium. This repulsive force can be mediated through either steric or electrostatic stabilization. Synthesized NPs have well-defined shapes without aggregation. This is due to the strong interaction between the chemically bound capping agents which interacts with the tendency of NPs aggregate. Secondary metabolites present in plant extract forms a coat on the NPs to prevent it from agglutination thus stabilizes the NPs, hence acts as capping agents.[20]

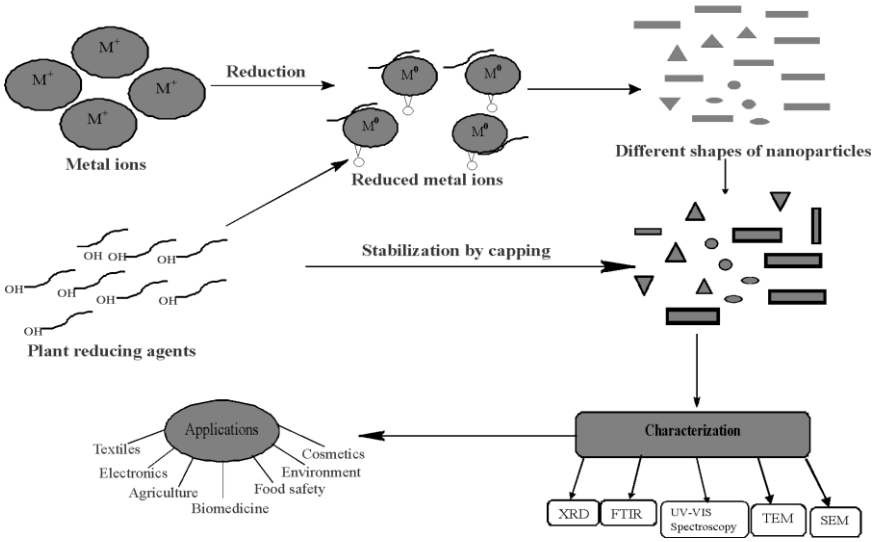

Figure 1.5 A hypothetical mechanism of plant-mediated synthesis of Ag NPs.[21,20]

The phenolic groups present in the plant extract subsequently undergo oxidation and get converted to their quinone forms. The electrochemical potential difference between Ag^+ and phytoconstituents drives the reaction. The formed Ag NPs are stabilized through the lone pairs of electrons and π-electrons of quinone structures.[22]

1.8 Factors Affecting the Formation of Ag NPs

Different parameters and reaction conditions such as temperature, pH, solvent medium, stirring time and reducing agents, etc. play a vital role for the greater stability, high yield, and controlled size and shape morphology in the context of green nanotechnology.[23,24]

pH is one of the most important factors influencing the synthesis of different NPs at different intervals depending upon plant species or microorganisms. Synthesized NPs are better stable in basic medium [25,26] with rapid growth rate, good yield, monodispersity, and enhanced reduction process. However, at acidic pH values, nanoparticles aggregation is dominant over the process of reduction.[17] Small and uniform-sized NPs were synthesized by increasing the pH of the reaction mixture.[27] However, very high pH (pH>11) leads to the formation of agglomerated and unstable Ag NPs.[28]

Temperature plays an important role in the synthesis of nanoparticles. Depending on biopolymers and plant extracts, temperatures up to 100 °C were mostly used for Ag NPs synthesis. The broadening peak obtained at low temperature shows the formation of large-sized NPs and the narrow peak obtained at high temperature, indicates the NPs synthesized are smaller in size. Although the higher temperature is optimum for NPs synthesis,[29] it has been found that elevated temperature increases its size due to an increase in fusion efficiency of metal ions which dematerialize supersaturation.[20] With the increase in the incubation period time, the stability of Ag NPs also increases.[30,31] Similarly, other conditions, such as concentrations of salt and reducing and capping agents and localizations for NPs synthesis depends on species and extracts, to create NPs with homogenous size and morphology.

1.9 Applications of Ag NPs

The unique physical, chemical and mechanical properties of Ag NPs have led to be used for numerous applications like medical, environmental, consumer

goods and personal care, food, electronic components and transportation, catalysis, antibacterial, antimicrobial, antiviral, anti-larvicidal, and antifungal activity.[14]

1.10 Use of Ag NPs in the Detection of Malathion

One of the major problems people are facing nowadays arises from the overuse of pesticides. Excessive use of pesticides has resulted in serious contamination of air, water, and land, thereby posing threat to the environment as well as human health.

Organophosphorus pesticides (OPPs) are the most extensively used pesticides in agriculture due to their relatively low persistence under natural conditions and high effectiveness for insect eradication. They are cholinesterase inhibitors that inhibit acetylcholinesterase (AChE), which acts as a neurotransmitter both in the central nervous system and in the nerve skeletal muscle junction. As a result, accumulation of the acetylcholine (ACh) neurotransmitter occurs and, thus terminates the transmission signal on postsynaptic cholinergic receptors leading to rapid paralysis of vital functions in living beings, interfering with muscular responses and causing respiratory and myocardial malfunctions and even death.[32,33]

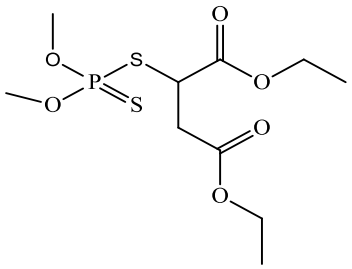

Figure 1.6 Structure of malathion

Malathion is one of the most widely employed organophosphate insecticides in agriculture as well as residential areas. Its adverse effects on human health include numbness, decreased coordination, dizziness, tremor, nausea, blurred vision, difficulty in breathing, slow heartbeat, headache, and tingling sensations. It is slightly toxic to mammals, moderately toxic to birds, and highly toxic to aquatic organisms, both freshwater and estuarine, as well as bees. Therefore, its detection even in trace amounts is very important from an environmental point of view. Hence, it has been very necessary to develop simple, rapid, reliable,

accurate yet sensitive approaches for the detection of malathion which is served by the field of nanotechnology. In this study, we have used modified green Ag NPs (L-cys-Ag NPs) as a colorimetric sensor to detect malathion.

1.11 Toxicity of Ag NPs

Though Ag NPs have been widely used for many applications throughout the world, various studies and reports revealed that nanosilver can allegedly cause adverse effects on humans as well as environments.[34] Tones of silver are released in free ions form into the environment from industrial wastes whose adverse effects on humans and all living beings include permanent bluish-grey discoloration of the skin (argyria) or eyes (argyrosis).[35] According to *in vitro* studies report, Ag NPs produced toxicity that targeted a variety of organs including the lung, liver, brain, vascular system, and reproductive organs. Studies also suggest that the "aged" (immersed) nanosilver is more toxic than the new nanosilver.[36]

Some investigations reported that there is an optimal size for efficient endocytosis of nanomaterials, independent of the particle composition. The synthesis approach and methodology used to produce nanomaterials is another factor that determines the toxicity.[37] Metallic silver appears to pose minimal risk to health and there are several permissible exposure limits (PELs) and guidelines exist for silver. The American Conference of Governmental Industrial Hygienists has established separate threshold limit values for metallic silver (0.1 mg/m^3) and soluble compounds of silver (0.01 mg/m^3). On the other hand, the exposure limit for all forms of silver is 0.01 mg/m^3 as recommended by The National Institute for Occupational Safety and Health. Thus, many researchers have recommended that separate PELs be established.[35] Though these studies tend to suggest that nanosilver can induce toxicity to living beings, it has to be understood that the studies on nanosilver toxicity were done in *in-vitro* conditions which are drastically different from *in-vivo* conditions and at quite high concentrations of nanosilver particles. So, we can employ a green synthesis method to deliver safer Ag NPs. For the welfare of lives, more studies are essential to be carried out to assess the toxicity effects in *in-vivo* conditions and derive a conclusion.

1.12 Mechanism of NP-based Colorimetric Sensors

Colorimetric sensors are constructed based on the intrinsic character of NPs which color will change upon the addition of a specific analyte.[38] NPs exhibit specific optical characteristics in the visible region. Localized surface plasmon resonance (LSPR) is a result of the confinement of surface plasmons in NPs with dimensions smaller than the wavelength of the incident light. Their properties have a strong impact on the resonance frequency and the intensity of the surface plasmon absorption bands.[39]

The main mechanisms behind the use of NPs in the detection and determination of target substances are that these NPs are sensitive to changes of the analyte at a very low level.[40] When the NPs are influenced by electromagnetic radiation, the electrons of the atoms in NPs surface can easily move through vacant orbitals and then generate absorption at a particular wavelength. This characteristic plays a critical role in colorimetric sensing.[38]

The mechanism lies in the aggregation due to the cross-linking or electrostatic adsorption.[41] Optical absorption can be strongly affected by both the distances and surface plasmon coupling in NPs, which would lead to the detection of a target in a simple colorimetric or visual manner.[42] The analyte would interact with the NPs by hydrogen bonding or electrostatic interactions and cause the aggregation of the NPs. The type and concentration of the analyte could affect the extent of aggregation, which is reflected by the degree of color change, usually measured by the UV-vis spectrophotometer.

1.13 Description of the Plant (*Parmelia sulcata Taylor*)

Figure 1.7 *Parmelia sulcata Taylor*

Parmelia sulcata Taylor (Parmeliaceae) is a foliose lichen commonly found from temperate to cold regions of both the Northern and Southern Hemispheres. In Nepali, lichens are commonly known as Jhayaoo or Tare. It was first described by Taylor (1836) from Ireland, is characterized by squarrose rhizines.[43] It contains atranorin, chloroatranorin, salazinic acid, and protocetraric acid.[44] Very little work has been done on it in Nepal till now. So its further exploration and study are felt as an important aspect.

CHAPTER II

OBJECTIVES OF THE STUDY

2.1 General Objectives

- To synthesize Ag NPs using *Parmelia sulcata Tayl*. extract and aqueous silver nitrate as a precursor and modify it by L-cysteine solution
- To use modified Ag NPs as a colorimetric sensor for organophosphorus pesticide (malathion) detection

2.2 Specific Objectives

- To characterize synthesized Ag NPs using Ultraviolet-visible (UV-vis) spectroscopy, X-ray diffraction (XRD), Scanning electron microscopy (SEM), and Energy dispersive X-ray analysis (EDX)
- To study the role of different pH on the green synthesis of Ag NPs and also its stability
- To determine the concentration of organophosphorus pesticide (malathion) by modified green Ag NPs
- To reduce the adverse effects of malathion on human health as well as on the environment by identifying its presence in various fruits and vegetables
- To make people aware of the adverse effects of excessive use of malathion

CHAPTER III

LITERATURE REVIEW

Various analytical methods have been developed and reported in the literature of OPPs like capillary electrophoresis, biosensor, colorimetric, immunochemistry, potentiometry, etc.[45] Among these methods, the colorimetric assay is a promising alternative to conventional techniques based on the determination of a measurable color change in the presence of target analytes. Nanotechnology-based approaches have attracted global attention in recent times for the detection, degradation, and removal of hazardous pesticides. Ag NPs of different sizes possess unique optical properties which lead to the detection of various pesticides. Their surface modification enhances the sensitivity and specificity of the pesticides.

To design a typical colorimetric sensor, we must have an idea regarding the proper ligand which can modify Ag NPs.[46]

Dubas and Pimpan (2008) have synthesized Ag NPs using the reducing agent of humic acid and its utilization for herbicide detection. The HA protected NPs were found to be sensitive to increasing concentrations of sulfurazon-ethyl herbicide in solution which induced a variation in color of the NPs solution from yellow to purple. An average Ag NPs size of 5 nm was confirmed by TEM.[47]

Xiong and Li (2008) reported a simple and effective colorimetric assay based on calixarene modified Ag NPs (pSCn-Ag NPs) for the determination of optunal. Calixarene molecules are non-toxic and have a high propensity to bind with aromatic amino rings. The optunal has an aromatic ring in their structure which easily binds to the pSCn-Ag NPs surfaces, inducing aggregation followed by a color change from yellow to red. The proposed colorimetric method shown an excellent detection limit of 10^{-7} M. The selectivity and sensitivity of pSCn-Ag NPs based assay was evaluated using other similar interferant pesticides including pyrimethanil, methomyl, thiabendazole, parathion-methyl, iprodione, acetamiprid. The obtained results suggested that the pSCn-Ag NPs only aggregate in the presence of optunal and no other significant change was noticed in the presence of other interferant pesticides. Furthermore, the developed sensor is effectively used for the determination of the optunal in real water

samples, and the results are correlated with the results obtained from the HPLC analysis.[48]

Lisha *et al*., (2009) reported colorimetric assays for chlorpyrifos and malathion in various water using citrate-capped Au NPs. Sodium sulfate was added to enhance the color change occurring by the adsorption of these pesticides on citrate-capped Au NPs. It can be easily aggregated by the addition of sulfur-containing OPPs because of the strong Au-S bond. However, its selectivity commonly lacks towards some OPPs because the method involves the formation of Au-S bond that may be formed with any sulfur-containing OPPs.[49]

Chai *et al*., (2010) developed Au NPs functionalized by L-cysteine for the Hg^{2+} colorimetric detection stimulated by ultraviolet light. The L-cysteine modified Au NPs induced aggregation quickly in the presence of Hg^{2+}, especially with the assistance of ultraviolet radiation. It showed relatively good selectivity for Hg^{2+} over other divalent metal ions with a detection limit (LOD) of 100 nM.[50]

Park *et al*., (2011) developed green synthesized Au NPs using heparin as a bio-reducing agent source from animal tissues for malathion, fenthion, and methidathion. Heparin possesses many negative charges compared to other polysaccharides and contributes to colloidal stability. Besides, the many hydroxyl groups and a hemiacetal reducing end of heparin may contribute to a reduction of Au salts. NaCl was used as a stimulator and induced a color change in the mixed solution from wine-red to purple-blue that was dependent on the pesticide concentration in the range of 10-1000 ppb. Au NPs-immobilized silica gel columns were successfully applied for removing fenthion in water confirmed by RP-HPLC and FTIR analyses.[51]

Zheng *et al*., (2013) proposed a rapid colorimetric assay based on cysteamine modified Au NP for recognition of glyphosate in water and environmental samples. The detection method is based on the accumulation of CS-Au NPs through electrostatic interaction in the presence of glyphosate which induced color change from red to blue. The developed assay showed an excellent analytical efficiency with a LOD of 5.88×10^{-8} M.[52]

Menon *et al*., (2013) developed a sensible and reliable approach for the recognition of dimethoate pesticides in industrial wastewater by using p-sulphonate Calix resorcinarene (pSC4R) modified metallic Ag NPs. The chemical principle for recognition of dimethoate is based on the π-π and

electrostatic interactions between nanoparticle surfaces and dimethoate, inducing aggregation resulting in a color change from yellow to red which can be monitored using the naked eye and the amount of dimethoate in the sample was estimated by using UV-vis spectroscopy. Moreover, the selectivity and affectability of the developed pSC4R- Ag NPs based assay was evaluated by adding some possible interferant pesticides. The sample containing dimethoate exhibited yellow to red color whereas no color or spectral change was noticed in the presence of other interfering substances. These results showed that the developed pSC4R-Ag NPs based colorimetric sensor has enormous potential for recognition of dimethoate in industrial wastewater samples although more work has to be done for its determination from food matrix.[53]

Vasimalai and John (2013) used chitosan capped Ag NPs as fluorophore for ultrasensitive and selective determination of malathion. The Chi-Ag NPs showed the absorption maximum at 394 nm and emission maximum at 536 nm. Based on the decrease in emission intensity, the concentration of malathion was determined. The lowest LOD was found to be 94 fM L^{-1}. The presence of 1000-fold common interferences such as chlorpyrifos, methyl parathion, endosulfon, imidacloprid, and alphamethrin do not interfere in the determination of 10 nm malathion. The proposed method was successfully applied for the determination of malathion in water and fruit samples. Further, the results obtained from the present method were validated with the HPLC method.[54]

D'Souza *et al*., (2014) used ascorbic acid (A A) to cap Au NPs (A A-Au NPs) for detecting dichlorvos in wheat samples, water (tap, river, and canal), and apple. Dichlorvos induced aggregation of A-Au NPs through hydrogen bonding, which results in a broader wavelength (620 nm) and transition color from cherry-red to purple. This is due to oxidized molecules with two hydroxyl (-OH) groups have created favorable sites for four oxygen-containing groups of dichlorvos to form extended arrays of hydrogen-bonding. The LOD of this method was reported as 42.94 μM. This method is restricted to the samples which contain only 1.0 mM of interfering pesticides (acephate, monocrotophos, chlorpyrifos, quinalphos, triaxophos, glyphosate, thiram, indoxacarb, fenvalerate, matalaxyl, and mancozeb). Otherwise, dilution of a sample should be performed to eliminate the interference.[55]

Wang *et al*., (2014) synthesized lanthanum functionalized Au NPs (La-Au NPs) for the determination of methyl parathion in river water and soil samples. Noteworthy, this highly sensitive approach is the first application using Au NPs based colorimetric assay that involved new type crosslinking molecules La^{3+} with OPPs due to strong coordination effect on oxygen-containing functional groups. In this study, lanthanum acts as a molecular bridge between Au NPs and methyl parathion. Lanthanum in absence of methyl parathion may also induce NPs aggregation owing to its strong coordination integration between lanthanum and citrate stabilized AuNPs without changing the color of the solution. In the presence of methyl parathion, crosslinked molecules $La^{3+}$with methyl parathion happens to experience a distinct color change (red to blue) that lead to the quantification of methyl parathion with good selectivity and sensitivity having LOD of 0.1 nM that is relatively low than traditional methods.[56]

Li *et al*., (2014) synthesized citrate capped Ag NPs and were used for the detection of dipterex in different water samples. These citrate-capped Ag NPs with immobilized acetylcholinesterase formed pink-colored aggregates due to the formation of thiocholine from acetylthiocholine through the enzymatic action of acetylcholinesterase. Dipterex inhibits the enzymatic action of acetylcholinesterase, due to which, there was no formation of thiocholine which allowed the bright yellow, Ag NPs to remain free with a characteristic absorbance at 400 nm.[57]

Liu *et al*., (2015) reported a method for the determination of the herbicide atrazine in tap water samples using melamine modified Au NPs (Mel-Au NPs). When atrazine was added to the solution was added to Mel-Au NPs, the color changed from wine-red to blue due to a transition from monodisperse to aggregated Mel-Au NPs caused by strong hydrogen bonding between atrazine and melamine. Although the LOD of atrazine is as low as 16.5 nM, however the presence of Pb^{2+} and Hg^{2+} (20 μM) can interfere with the determination of atrazine. Thus, pre-treatment of real samples using EDTA to remove the heavy metals is needed.[58]

Kodir *et al*., (2016) developed a pesticide colorimetric sensor based on Ag NPs modified by L-cysteine. Pesticides namely monosultap and cypermethrin, were detected by mixing them with Ag NPs. The fresh L-cys-Ag NPs had brownish

yellow color in as much as surface plasmon resonance absorbance centered at 422 nm. NaCl stimulated color change from brownish yellow to clear which was relied on pesticide concentration of 20, 50, and 100 ppm. In the presence of cypermethrin, L-cys-Ag NPs color turned clear and the peak absorbance dropped to 0.17 from 1.15. However, the effect of monosultap toward L-cys-Ag NPs was negligible.[59]

Bala *et al*., (2016) employed aptamer, cationic peptide, and unmodified Au NPs for the detection of malathion in environmental samples. The color of the NPs remained red in the absence of malathion as the peptide is bound to the aptamer whereas in the presence of malathion, the aptamer is linked to malathion and the peptide is free to cause the aggregation of particles changing the color to blue. The results demonstrated that a hexapeptide i.e., KRKRKR can also be easily employed for highly sensitive and rapid monitoring of malathion in real samples. It utilized the optical changes of the Au NPs for the colorimetric detection of malathion. It was found to be linear in the range of 0.01-0.75 nM with a LOD of 1.94 pM which is significantly lower than the other available reports.[60]

Wu *et al*., (2017) developed a novel colorimetric method for highly sensitive detection of OPPs in aqueous media based on the enzymatic hydrolysis reaction of AChE and the dissolution of Au NPs in Au^{3+}-cetyltrimethylammonium bromide (Au^{3+}-CTAB) solution. In the absence of OPPs, the enzymatic hydrolysis product, thiocholine, reduced Au^{3+} and protected the Au NPs from dissolution by the Au^{3+}-CTAB. In the presence of OPPs, however, the activity of AChE is inhibited, which could not or could only produce a small amount of thiocholine to consume the Au^{3+}. In this case, the large amount of residual Au^{3+} dissolved the Au NPs and decreased both the concentration and size of the Au NPs, thus leading to an obvious red-to-light pink or red-to-colorless color change. This method exhibited high sensitivity and good tolerance to high salinity, which could detect parathion with concentration down to 0.7 ppb and be performed in seawater. After loading Au NPs on a cellulose paper, an Au NPs-coated dipstick is developed for the detection of OPPs, which is highly sensitive with an observable limit of detection of 35 ppb.[61]

Siangproh *et al*., (2017) synthesized Ag NPs to detect paraquat using a colorimetric assay in canal water, groundwater, green apple, and Chinese

cabbage. The detection mechanism involved the color change from yellowish-green to pale yellow because of the accumulation of anionic Ag NPs in the existence of paraquat.[62]

Luo *et al*., (2017) synthesized Ag NPs modified with rhodamine B (RB)and used them to detect carbaryl in tomato, apple, and river water. This pesticide detection was based on colorimetric and fluorescence assay. The enzymatic action of acetylcholinesterase on the substrate formed thiocholine, which converted the yellow solution of RB-Ag NPs to grey. Simultaneously, the fluorescence of RB was also unquenched. In the presence of pesticide, no color change or fluorescence was observed, which confirmed the presence of pesticide in the sample.[63]

Liou *et al*., (2017) synthesized Ag NPs coated on cellulose nanofibers to develop the SERS platform for the detection of thiabendazole (TBZ) in apples. TBZ is a neutral and hydrophobic molecule that has a low affinity for the surface of negatively charged Ag NPs. Therefore, TBZ only exhibited strong SERS signals when the pH is below the TBZ's pk_a value (pH=4.65) based on the electrostatic attractions between Ag NPs and TBZ. These nanofibers helped in preventing the aggregation of Ag NPs, thus avoiding any deviations in the Raman signals from the pesticides.[64]

Chen *et al*., (2018) reported a colorimetric method for the determination of dimethoate (DMT) and terbuthylazine (TBA) pesticides in water and food samples using citrate-stabilized Au NPs. It is dependent upon the aggregation and anti-aggregation of Au NPs in the presence of NaOH. At a low concentration of alkali, Au NPs are well-dispersed (wine-red) due to electrostatic repulsion while Au NPs are aggregated at a high concentration of alkali with the color change from red to grey. The LOD of this assay for terbuthylazine and dimethoate was reported at 0.3 μM to 20 nM by naked eyes and 0.02 μM and 6.2 nM using UV-vis spectrophotometer. Along with this, 30 types of potential interferant substances have been analyzed to access the selectivity and sensitivity of the developed assay.[65]

Wang *et al*., (2018) proposed a fast-colorimetric technique for the identification of deltamethrin using 2-mercapto-6-nitro-benzothiazole modified Au NPs (MNBT-Au NPs). Deltamethrin easily sticks to MNBT-Au NP surfaces and formed a core-shell structure in which MNBT-Au NPs serve as the core and

deltamethrin as the shell. The formation of the core-shell structure facilitated the aggregation of MNBT-Au NPs leading to color change from red to purple. The color change was noticed using a bare eye and the quantity of deltamethrin in the sample was estimated by UV-vis spectroscopy. The analytical efficiency for deltamethrin was reported at 0.25 μM with bare eyes and 0.005 μM using UV-vis spectroscopy. This approach was successfully used for the recognition of deltamethrin in real samples of cherries and tomatoes. The obtained results were consistent with the results obtained from GC-MS analysis, suggesting that the proposed sensor had enormous potential for onsite detection of deltamethrin.[66]

Kang *et al*., (2018) developed a sensitive method for colorimetric determination of pymetrozine in water, apple, and green tea samples using melamine-modified Au NPs (M-Au NPs). The chemistry behind this assay is based on the fact that melamine has three amine groups in its structure, which constitutes a strong hydrogen bonding with pymetrozine that induces aggregation of M-Au NPs. Therefore, when the pymetrozine solution was added to the M-Au NPs solution, a change in color from red to blue was observed. The developed colorimetric sensor showed a high affinity towards pymetrozine in the presence of other pesticides. The LOD was reported at 80 nM with naked eyes and 10 nM using UV-vis spectrophotometer which is better than other existing instrumental methods.[67]

Ma *et al*., (2018) constructed an ultrasensitive assay for quantitation of trizophos via aggregation of citrate capped Ag NPs. The mechanism behind this assay is based on the π-π interaction, hydrogen and electrostatic bonding between citrate ions and trizophos leads to aggregation and change in color of Ag NPs from bright yellow to red-brown demonstrating an excellent analytical efficiency with LOD of 5 nm. The real water and fruit samples were analyzed to access the applicability and accuracy of the proposed sensor.[68]

Rana *et al*., (2018) developed a strategy for colorimetric identification of six pesticides (Acephate, Acetamiprid, Phenthoate, Profenofos, Cartap, Chlorothalonil) in drinking water and vegetable samples using citrate-Au NPs. The detection mechanism is based on the ligand exchange and electrochemical reactions between the nanoparticle's surfaces and target pesticides. Under optimized conditions, a color change from red to blue was observed when the

solutions of target pesticides were added to citrate-Au NPs. The selectivity and sensibility of the developed sensor were estimated with the presence of possible interferant substances including metal ions, anions, and other pesticides. The results showed that no significant change in color or LSPR was noticed, indicating the high selectivity and sensitivity of the developed assay. Although, the detection phenomenon is influenced by the medium pH so the appropriate pH of the medium is crucial for detection of all target pesticides.[69]

Singhal and Lind (2018) developed a new method for the one-step synthesis of cysteine-capped Ag NPs. Characterization of the synthesized NPs was done by several techniques, including UV-vis spectroscopy, IR spectroscopy, X-ray diffraction, SEM, and TEM. The interaction of these NPs had been seen with two pesticides, namely, chlorpyrifos and malathion. Chlorpyrifos had a better affinity to Ag NPs compared with malathion due to the aromatic amine group present in chlorpyrifos as evidenced by IR. Chlorpyrifos followed second-order kinetics whereas malathion followed interparticle diffusion. According to this study, Ag NPs are not very active to malathion but is a better choice to remove chlorpyrifos from the drinking water.[70]

Abnous *et al*., (2018) described a method for the colorimetric determination of the pesticide malathion based on the use of a hairpin structure consisting of a complementary strand of aptamer and a double-stranded DNA (dsDNA) structure to protect Au NPs against salt-induced aggregation. In the absence of malathion, the dsDNA structure was preserved on the surface of Au NPs and the color of the Au NPs in solutions containing NaCl remained red. However, in the presence of malathion, a hairpin structure of the complementary strand was formed. The Aptamer/Malathion complex and the complementary strand were released from Au NPs surface. As a result, Au NPs undergo salt-induced aggregation followed by a color change to blue. This assay indicated a low LOD of 1 pM and high specificity for malathion and successfully applied for detection of malathion in serum samples.[71]

Li *et al*., (2019) developed a highly sensitive and adaptive approach for visual determination of malathion using the anti-aggregation phenomenon of Au NPs. The colloidal Au NPs are wine-red and under alkaline conditions (pH > 9) the color of the Au NPs was changed from wine-red to grey. Under alkaline conditions, malathion undergoes simple hydrolysis producing a strong negative

charge and changed the color of aggregated NPs from grey to red. This probe exhibited a linear response to malathion in the concentration range of 0.05-0.8 μM with a limit of detection (LOD) down to 11.8 nM with a recovery of 94-107% and a relative standard deviation (RSD) less than 8%.[72]

Similarly, Ghoto *et al*., (2019) led a sensitive approach for the identification of dithiocarbamate pesticides (ziram, nabam, and maneb) using sodium dodecyl sulfate capped Ag NPs in real tap water, tomato, and mango samples. The interaction between the sulfate group of SDS-Ag NPs and the amino group of dithiocarbamate pesticides induced aggregation and results change in color of SDS-Ag NPs solution from yellow to dark brown. The detection limit of this assay was reported at 4.0, 9.1, and 149.3 ng/ml for zineb, maneb, and ziram, respectively.[73]

Khalkho *et al*., (2020) developed a highly selective and sensitive colorimetric probe for the determination of vitamin B1 using cys-capped Ag NPs as a chemical sensor. The sensitivity of the colorimetric assay is based on the LSPR band changes in the region of 200-800 nm and aggregation of cys-capped Ag NPs upon the successive addition of vitamin B1 in the presence of potentially interfering chemical substances including other vitamins. The electrostatic interaction among negatively charged cys-capped Ag NPs and positively charged vitamin B1 was theoretically explored by density function theory (DFT) using Gaussian 09 (C.01) program. The morphology, size distribution, and optical properties of cys-capped Ag NPs were characterized by TEM, UV-vis spectrophotometry, FTIR, and dynamic light scattering (DLS) techniques. The method is linear in the range of 25-500 μg mL^{-1} with correlation coefficient (R^2) 0.992 and LOD of 7.0 μg mL^{-1}. This colorimetric assay is promising for vitamin B1 detection from food (peas, grapes, and tomato) and environmental water samples.[74]

CHAPTER IV

EXPERIMENTAL METHODS

4.1 Collection and Identification of Plant Material

Lichen species were collected from Daman. Plant samples were identified and authenticated by Taxonomists from National Herbarium and Plant Laboratories (NHPL) located in Godawari-5, Lalitpur. The collected lichen was washed with sterile double distilled water and was air-dried. After that it was coarsely powdered by using a mechanical grinder. This powder was collected in a plastic bag and stored in a cool and dry place until used for further experiment.

4.2 Instrumentation

Mechanical grinder, digital weighing balance, magnetic stirrer, vortex, centrifuge (SORVALL ST 8R Centrifuge), incubator (1B-01E Incubator, Jeio Tech), UV-visible spectrophotometer (SPECORD 200 PLUS, analytikjena, Germany), X-ray diffraction (XRD), Scanning electron microscopy (SEM), Energy dispersive X-ray (EDX) were used during this work.

4.3 Solvents and Chemicals

Silver nitrate (Merck), sodium hydroxide (Fischer Scientific), L-cysteine (HiMedia), distilled water, Whatman filter paper 1, ethanol (Absolute ethanol 99.9%), and malathion (1000 ppm).

4.4 Preparation of Plant Extract by Boiling Method

1 g of lichen powder was boiled in 50 mL distilled water for 10 minutes in a beaker. After cooling, it was filtered through Whatman No. 1 filter paper. The filtrate was used for the experiment and the remaining extract was stored in the refrigerator at 4°C for further experiment. The obtained filtrate is called plant extract.

Figure 4.1 Preparation of lichen extract

4.5 Preparation of Silver Nitrate solution

A stock solution of $AgNO_3$ of 50 mM in distilled water was prepared by dissolving 4.2468 g of the compound in 500 mL distilled water. The stock solution was then diluted to prepare a 1 mM concentration. The solution was kept away from direct reach of light by wrapping the volumetric flasks with black covering and were kept in a fridge.

The molecular weight of $AgNO_3$: 169.87 g

[Ag-107.87, N-14, O-16] = 107.87+14+ (16x3) =169.87 g

Therefore, the molar mass of $AgNO_3$ =169.87 g

Concentration	Volume	Required amount of $AgNO_3$
1000 mM	1000 mL	169.87 g
1 mM	1 mL	(169.87/1000000) = 0.00016987 g
50 mM	500 mL	(0.00016987 x 50 x 500) = 4.24675 g

4.6 Preparation of L-Cysteine Solution

1 mM of L-cysteine solution was prepared by dissolving 0.0121 g of L-cysteine in 100 mL distilled water and providing mild heat.

The molecular weight of $C_3H_7NO_2S$: 121.16 g

Therefore, the molar mass of L-cysteine = 121.16 g

Concentration	Volume	Required amount of L-cysteine
1000 mM	1000 mL	121.16 g
1 mM	100 mL	(121.16/10000) = 0.0121 g

The solution was stored at room temperature.

4.7 Green Synthesis of Silver Nanoparticles

In a usual reaction procedure, 100 mL of 1 mM $AgNO_3$ solution was mixed by 10 mL of lichen's infusion in two different beakers. One of the mixtures was then alkalized with 0.1 M sodium hydroxide to maintain pH while the other was left as it was. Then both were stirred for 2 hours and kept at room temperature for 24 hours. The formation of Ag NPs was confirmed by the change in color of the solution from light yellow to reddish-brown and UV-vis spectra were recorded.

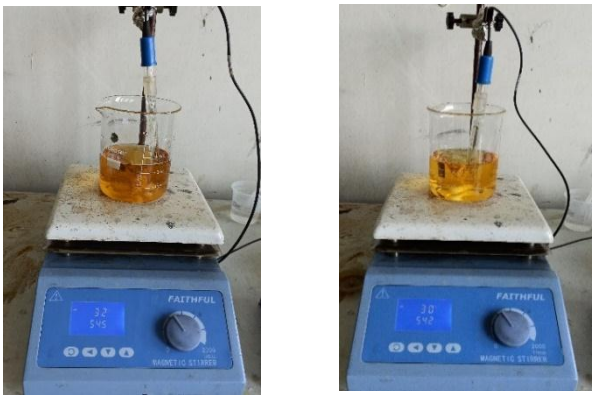

A B

Figure 4.2 Synthesis of Ag NPs (A) with NaOH and (B) without NaOH

The flow chart showing the green synthesis of Ag NPs is designed as below.

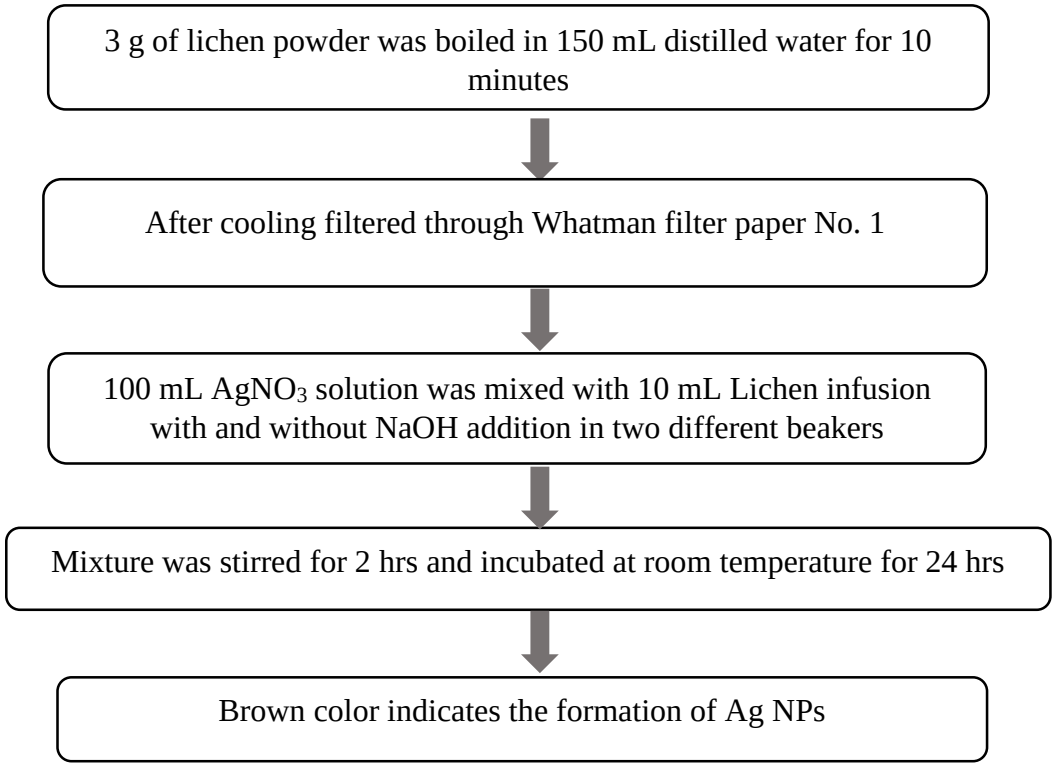

Figure 4.3 Schematic diagram of green synthesis of Ag NPs

4.8 Purification/Separation of Silver Nanoparticles

Ag NPs were separated by an ethanol precipitation method. The absolute alcohol was added into the fully reduced solution after 24 hrs. After centrifugation at 9000 rpm for 20 mins, Ag NPs were washed with ethanol thrice and after decanting, it was washed with distilled water three times. Then, the decanted solution was kept in an incubator and the same process repeated. The purified Ag NPs are then stored in an Eppendorf tube (airtight plastic tubes) covered with aluminum foil for further analysis.

4.9 Characterization Techniques

Characterization of NPs is important to understand and control NPs synthesis and applications. Various techniques are used for the determination of different parameters like particle size, shape, morphology, structure, crystallinity, pore size, fractional dimensions, surface chemistry, surface charge, dispersity, and surface area. Synthesized Ag NPs were characterized by UV-vis spectroscopy, X-ray diffraction (XRD), Scanning electron microscopy (SEM), and Energy dispersive X-ray analysis (EDX).

4.9.1 UV-Vis Spectroscopy

UV-vis Spectroscopy analysis was used to determine the absorption band and band gap which helps to confirm the formation of Ag NPs. The bio-reduction of pure Ag^{+} ions of each sample was monitored by the SPECORD 200 PLUS, analytikjena (An Endress+Hauser Company) UV/VIS Spectrophotometer. The scanning range for the samples was 300-700 nm at a medium scanning rate and resolution of 1 nm. Distilled water was used as a blank reference for the baseline correction of the spectrophotometer in the experiment. All the samples were loaded into 2 mL quartz cuvette with 1 cm path length for sampling.

4.9.2 X-Ray Diffraction (XRD)

Mainly, X-ray diffraction has been used for the fingerprint characterization of crystalline materials and the determination of their structure. Each crystalline solid has its unique characteristic X-ray diffraction pattern which may be used as a “fingerprint” for its identification. Once the material has been identified, X-ray crystallography may be used to determine its structure i.e., how the atoms pack together in a crystalline state and the interatomic distance and angle are,

etc. Here, X-ray diffraction gives information about the crystal structure of dried Ag NPs powder. Routine Powder X-ray diffraction patterns for dried Ag NPs were registered using the Rigaku D/MAX-2500/pc diffractometer with monochromated Cu Kα radiation of wavelength 1.54060 Å. The working conditions were typically 2θ scanning between 20° to 80°.

The crystallite size of the dried powder was determined from X-ray line broadening using Scherrer's equation as follows[75]

$$D = \frac{k\lambda}{\beta \cos \theta}$$

Where, D = crystallite or grain size,

k = dimensionless shape factor, with a value close to unity (0.9)

λ = wavelength of the radiation, (0.15406 nm for Cu Kα)

θ = Bragg's angle (half of the 2θ value of chosen peak), (should be in radians) and

β = full width at half maximum, FWHM (should be in radians)

4.9.3 Scanning Electron Microscopy (SEM)

Scanning electron micrograph measurements were employed to determine the high-resolution images of surfaces and the size of particles. The images were taken at Sun Moon University, the Republic of Korea.

4.9.4 Energy Dispersive X-Ray Measurement (EDX)

EDX is an analytical technique used for the elemental analysis or chemical composition of synthesized NPs. It is used to gain further insight into the features of Ag NPs. It was also carried out at Sun Moon University, the Republic of Korea.

4.10 Modification of Ag NPs Using L-Cysteine

3 mL of 1mM L-cysteine solution was blended with 165 mL of Ag NPs solution in a 1:55 volume ratio. The mixture was stirred for 30 minutes and then incubated for 24 hours since mixing time. Modified Ag NPs (L-cys-Ag NPs) solution was characterized by UV-visible spectrophotometer measuring optical absorbance and also photographic images were captured.

4.11 Detection of Organophosphorus Pesticide with L-Cys-Ag NPs

Standard malathion (1000 ppm) was diluted with distilled water to achieve a solution of 100 ppm, 10 ppm, 1 ppm, 0.1 ppm, and 0.01 ppm. Then 1 mL of L-cys-Ag NPs solution was mixed with 1 mL NaCl (1 M) solution and vortexed for 10 minutes before pesticide detection. After that, 1 mL of different concentration of malathion solution was added to above 2 mL Ag NPs and NaCl which showed color change. Then the resulting mixture was characterized using a UV-vis spectrophotometer and photographic images were captured.

CHAPTER V

RESULTS AND DISCUSSION

5.1 Study of Optical Properties Using UV-Vis Spectroscopy

When lichen extract was mixed with silver nitrate solution, it started to change the color from light yellow to brown due to the reduction of silver ion, which indicated the formation of Ag NPs. Characterization of synthesized Ag NPs was done by UV-vis spectrophotometer. The UV-vis spectra of lichen extract was also observed which is shown in figure 5.1.

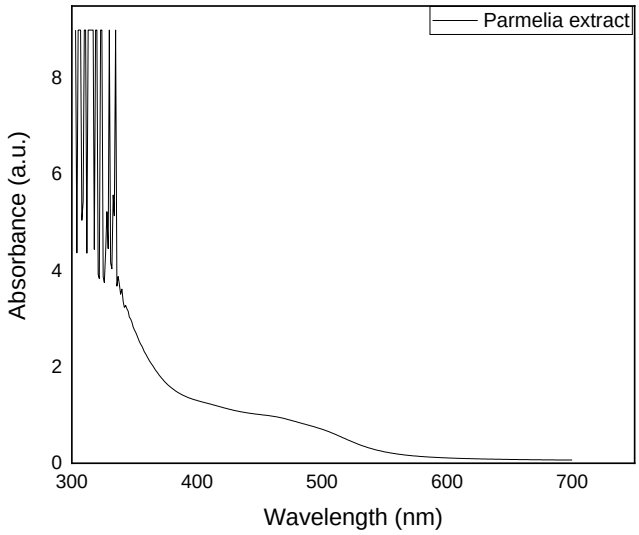

Figure 5.1 UV-vis spectra of lichen extract

Figure 5.2 showed the UV absorption peaks of Ag NPs with pH maintained at 429 nm and 428 nm in 2 hrs and 24 hrs respectively, clearly indicating the formation of spherical Ag NPs.[76] This is because at higher pH, the large number of functional groups available for silver binding facilitated a higher number of Ag NPs to bind and subsequently form a large number of NPs with smaller diameters. The UV absorption peak of Ag NPs range from 400-470 nm mostly. The occurrence of the peaks is due to the phenomenon of surface plasmon resonance (SPR), which occurs due to the excitation of the surface plasmons present on the outer surface of the Ag NPs that gets excited due to the applied electromagnetic field. The surface plasmon resonance bands are influenced by

the size, shape, morphology, composition and dielectric environment of the synthesized NPs.[77]

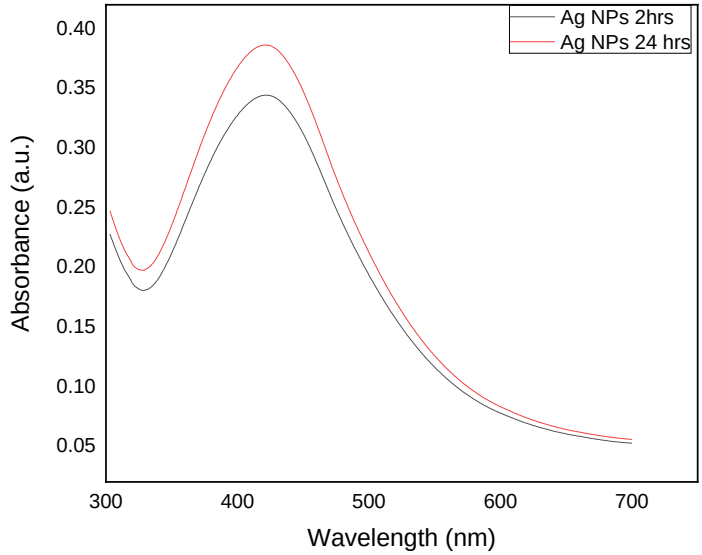

Figure 5.2 UV-vis spectra of Ag NPs after 2 hrs and 24 hrs at pH 10

Figure 5.3 Photographic images of Ag NPs after 24 hrs and 2 hrs at pH 10, lichen extract and $AgNO_3$

Figure 5.3 includes photographic images of Ag NPs, lichen extract and $AgNO_3$. Here the solution after 24 hrs (vial 1) was dark brownish in color compared to solution after 2 hrs (vial 2) which was brownish-yellow in color. This color change is due to the property of quantum confinement which is a size-dependent property of NPs affecting its optical properties. The brownish-yellow color in vials 2 and 1 confirmed that Ag NPs existed in the solution with an increase in absorbance from 0.3425 to 0.384. The intensity of brown color increased in direct proportion to the incubation period which may be due to the excitation of SPR effect and the reduction of $AgNO_3$.[78] Similarly, $AgNO_3$ solution (vial 4)

and lichen infusion (vial 3) had clear and pale-yellow color, respectively which was different from the solution of Ag NPs.

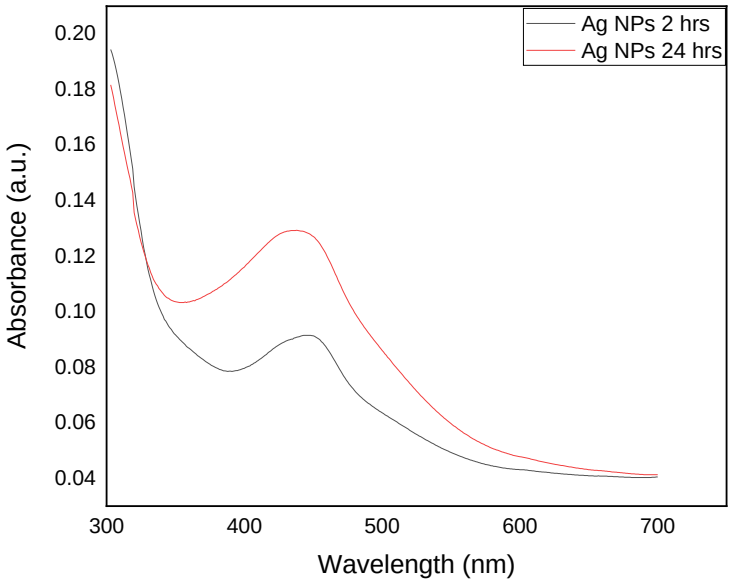

Figure 5.4 UV-vis spectra of Ag NPs (without NaOH) after 2 hrs and 24 hrs

Figure 5.4 shows the UV-vis spectra of Ag NPs recorded after 2 hrs and 24 hrs without addition of sodium hydroxide. Though the absorption peaks obtained at 447 nm after 2 hrs and 448 nm after 24 hrs respectively also confirmed the formation of Ag NPs but in this case aggregation is most likely to be favoured. This is because at low pH, the aggregation of Ag NPs is dominant over the nucleation to form larger nanoparticles.[17] Acidic condition suppresses the formation of Ag NPs, but the essential condition enhances its formation.[79] The increase in absorbance of Ag NPs from 0.0915 to 0.1278 with an increase in incubation period is also due to the excitation of SPR effect and the reduction of $AgNO_3$.[78] This was also confirmed by color of Ag NPs which was light yellowish-orange unlike orange lichen extract and clear $AgNO_3$ solution as shown in figure 5.5. The light yellowish-orange color of Ag NPs even after 24 hrs reported that lower pH affects its formation by favouring aggregation process, which in turn, affects its absorbance as well as intensity. This is the reason for the difference in absorbance, intensity and color of Ag NPs synthesized in the presence and absence of sodium hydroxide.

1 **2** **3** **4**

Figure 5.5 Photographic images of lichen extract, $AgNO_3$, Ag NPs (without NaOH) after 2 hrs and 24 hrs

5.2 Study of Crystal Structure of Ag NPs by X-Ray Diffraction

The XRD pattern of synthesized Ag NPs obtained by using an aqueous extract of *Parmelia sulcata* is shown in figure 5.6.

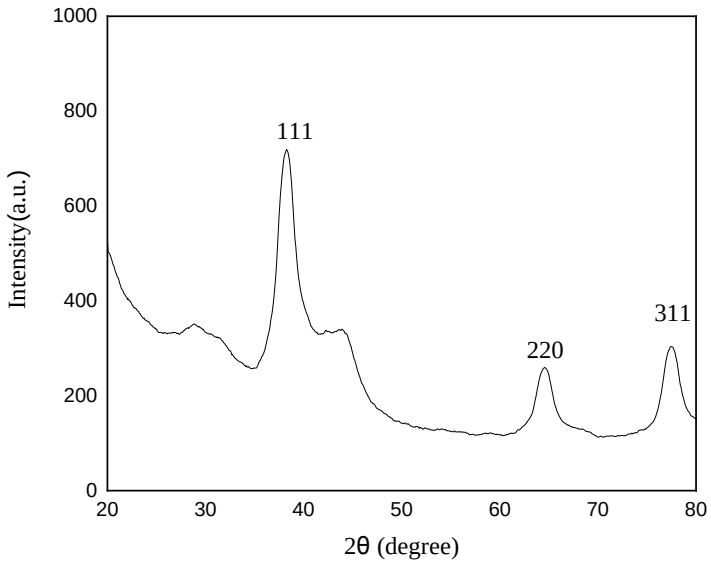

Figure 5.6 XRD of silver nanoparticles

All diffraction peaks correspond to the characteristic face-centered cubic (FCC) silver lines, which is in good agreement with the powder data of JCPDS Card number 04-0783. These diffraction lines observed at 2θ angle 38.20°, 64.54°, and 77.46° have been indexed as (111), (220), and (311) respectively. The XRD pattern thus clearly shows that Ag NPs formed by *Parmelia sulcata* are crystalline in nature. This result is consistent with the results reported by Jain *et*

al.,[80] Cruz *et al*.,[81] and Gilaki.[82] The other characteristic peak at 28.63° may be due to the crystalline nature of the bio-organic phase (capping agent) on the surface of the Ag NPs as well as may be silver oxide due to the partial oxidation of silver. The average crystallite size of the synthesized Ag NPs was calculated from the width of all diffraction peaks obtained by the Gaussian fitting of all four peaks using the Debye-Scherrer formula and it was found to be 7.46 nm.

The crystallite size of the dried powder was determined from X-ray line broadening using Scherrer's equation as given below:

$$D = \frac{k\lambda}{\beta \cos \theta}$$

Table 5.1 Calculation for Crystalline Size

Peak position (2θ)	FWHM	FWHM (β)	Crystallite size D (nm)	Average size (nm)
38.20298	1.3601	0.023738223	6.181299353	7.465469
64.54384	1.13248	0.019765505	8.296573299	
77.46094	1.28606	0.022445981	7.918533459	

5.3 Scanning Electron Microscopic Image

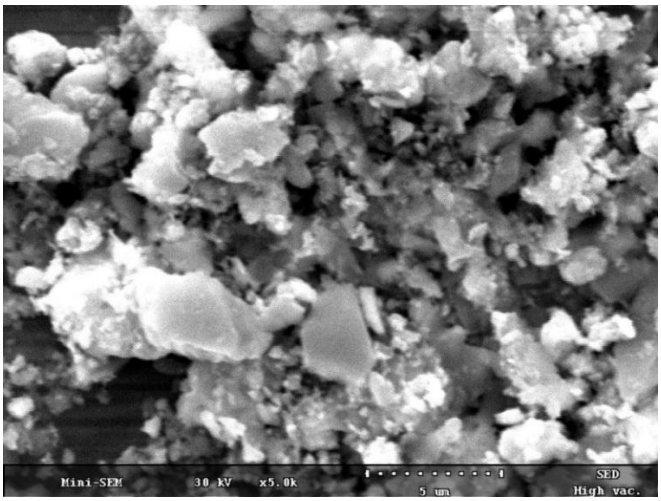

Figure 5.7 SEM images of silver nanoparticles under 5000 magnification

Figure 5.7 showed that the structure of Ag NPs has an irregular shape and some are agglomerated. Variable sizes of NPs were observed.

5.4 Energy Dispersive X-Ray Analysis

The reduction of silver ions to elemental silver by the aqueous extract of *Parmelia sulcata* was confirmed by Energy dispersive X-ray (Figure 5.8).

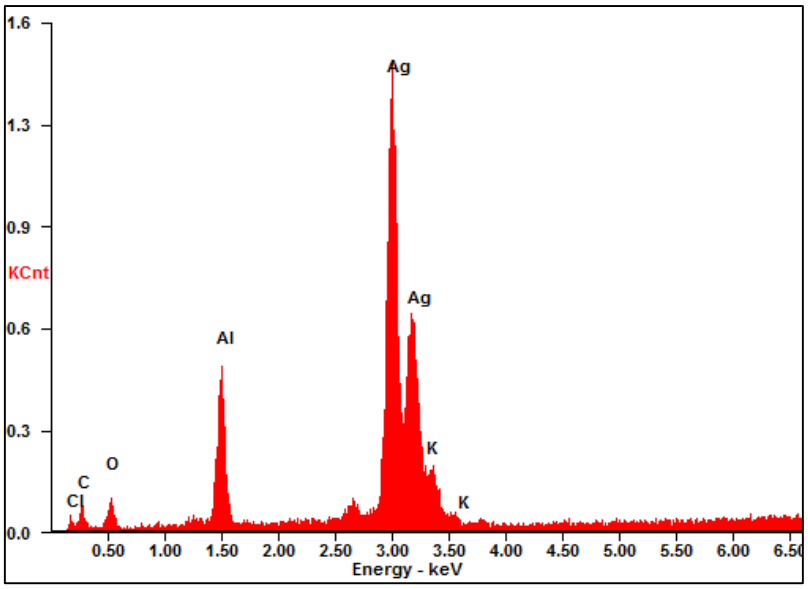

Figure 5.8 Energy dispersive spectrum of silver nanoparticles

EDX spectrum showed two sharp to moderate absorbance peaks of Ag with 1.5 and 0.7 scale counts corresponding to 3 and 3.2 keV respectively. The concentration of Ag was observed as 69.33 weight percentage and 27.94 atom percentages. The presence of other elements such as carbon, oxygen, aluminum, potassium, and chlorine was due to the elements present in lichen extract which may help in capping and stabilizing the Ag NPs.[83] The optical absorption peaks obtained at approximately 3 keV confirms the presence of nanocrystalline elemental Ag due to SPR effect.[84] The signals of carbon is due to the grid used for EDX spectra analysis and also the peaks of oxygen observed is mainly due to the oxidation of samples.[85] The *Parmelia sulcata* contains several metabolites, including atranorin, chloroatranorin, salazinic acid, and protocetraric acid that may play a significant role as reducing agents for silver ions.[44,86]

5.5 Modification of Ag NPs with L-Cysteine

As we can see in figure 5.9 below, modified Ag NPs (vial 3) showed an increased intensity of color which made it look darker compared to Ag NPs (vial 1) whereas L-cysteine solution was clear. This means that L-cysteine acts as a modifier and gave an impact to Ag NPs to form L-cys-Ag NPs.

Figure 5.9 Photographic images showing modification of Ag NPs with L-cysteine

If we talk about absorbance spectra as shown in figure 5.10, L-cysteine had no absorbance peak in the wavelength range of 300 nm-700 nm. Similarly, Ag NPs which initially had a peak absorbance of 0.1278 increased to 0.1581 after it was modified. Absorbance depends on the refractive index of NPs. The increasing absorbance means the increase of the refractive index of Ag NPs in the solution.[87] In this way, we could say that L-cysteine had successfully modified Ag NPs by increasing the refractive index.

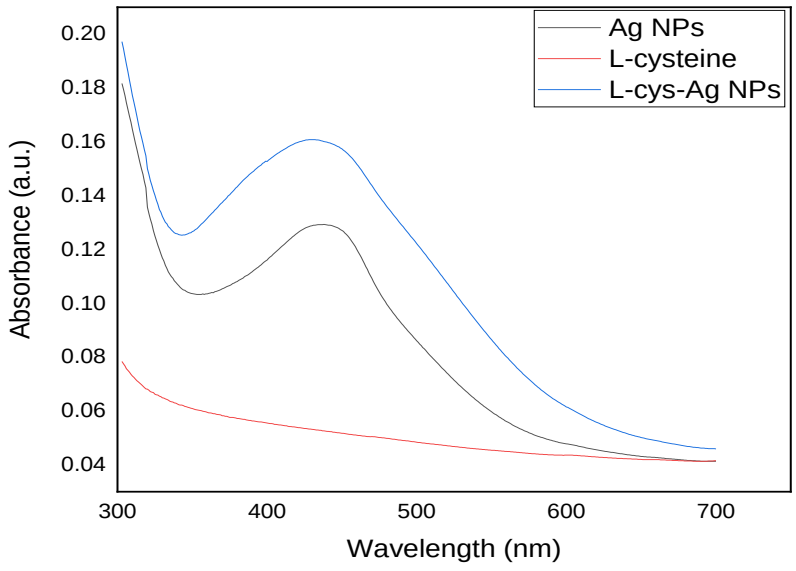

Figure 5.10 UV-vis spectra of modified Ag NPs with L-cysteine

5.6 Detection of Malathion with L-Cys-Ag NPs

I **II** **III** **IV** **V** **VI** **VII** **VIII**

Figure 5.11 Detection of different concentrations of malathion with L-cys-Ag NPs

As we can see the photographic images in figure 5.11, we could easily detect the color alteration of the solutions. Vial (II) which contained L-cys-Ag NPs was darker than vial (I) containing Ag NPs. L-cys-Ag NPs when mixed with NaCl changed its color from brown to yellow as shown in vial (III). Furthermore, solution containing Ag NPs and NaCl was mixed with different concentrations of malathion i.e., 100 ppm, 10 ppm, 1 ppm, 0.1 ppm and 0.01 ppm as shown in vial IV, V, VI, VII and VIII respectively. Upon the addition of increasing concentrations of malathion to L-cys-Ag NPs and NaCl solution, its SPR band is gradually decreased without change in the absorption wavelength maximum followed by color change from intense yellow to light yellow.

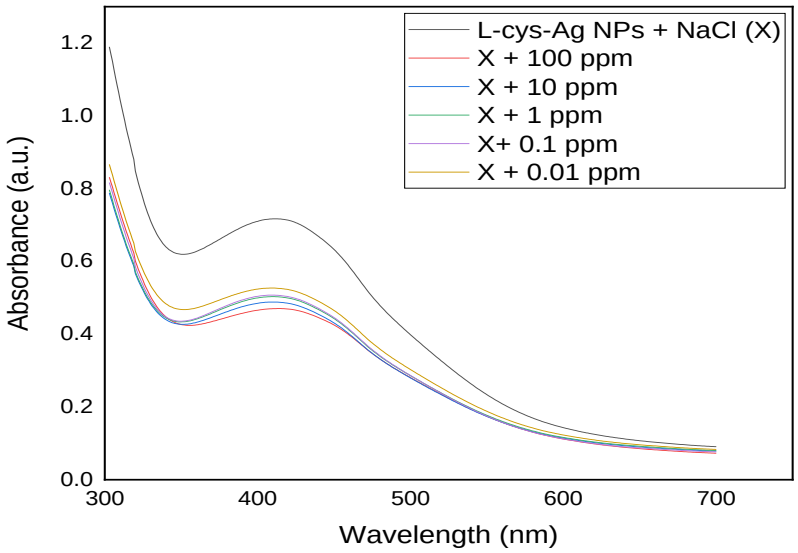

Figure 5.12 UV-vis spectra of L-cys-Ag NPs and NaCl (X) containing different concentrations of standard malathion

Figure 5.12 indicates the absorbance spectra of L-cys-Ag NPs and NaCl solution after the addition of different concentrations of malathion over 5 minutes.

As the pesticide concentration increased from 0.01 ppm to 100 ppm, the absorbance at 430 nm decreased. This means that the number of Ag NPs decreased because of Ag NPs aggregation. The more aggregation the fewer Ag NPs left leading to the decrease in absorbance. The observed spectral and color changes of L-cys-Ag NPs and NaCl solution is attributed to its interaction with malathion.

Zeta potential is the difference between tightly bound layer and electroneutral region. If the value of zeta potential is high, it influences to large distance and if its value is low, it influences to small distance. In this case L-cys-Ag NPs have disclosed COO^- outside which develops repulsive force among the negative charge COO^- groups of the L-cysteine molecules on the surface boundary hindering the formation aggregates. When it is mixed with NaCl solution, it bears positive charge and the electrostatic repulsion between the positive charges protects the Ag NPs from the aggregation. But when it is mixed

with pesticide, surface charge decreases due to its adsorption leading to decrease in distance of particles thereby causing aggregation.

With the increment in cationic concentrations such as Na^+ from NaCl and Ca^{2+} from $CaCl_2$, the aggregation rate of L-cys-Ag NPs also increases.[88]

Malathion undergoes hydrolysis in acidic pH as given below:

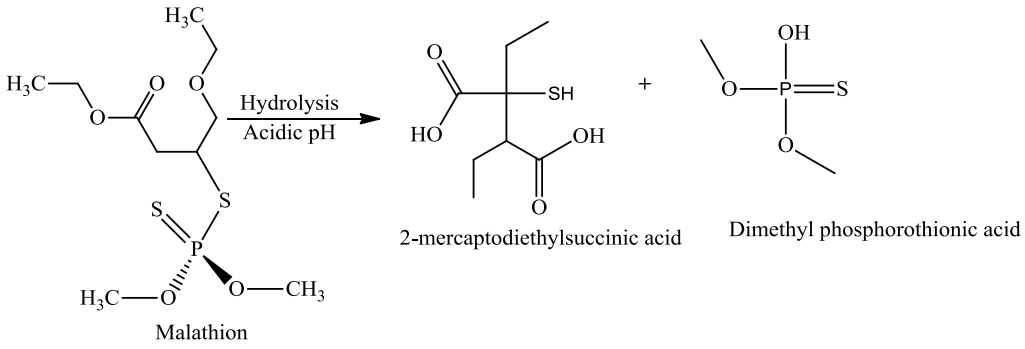

Figure 5.13 Hydrolysis of malathion in acidic pH[89]

The hydrolysis products of malathion are dimethyl phosphorothionic acid and 2-mercaptodiethylsuccinic acid. Steiner (2002) reported that the acidic -OH group of 2-mercaptodiethylsuccinic acid and phosphorothionic acid has the hydrogen bonding interaction with -OH group of chitosan.[90,91] Thus this interaction may also be possible with L-cysteine.

L-cysteine is a sulfur-containing amino acid. It is easily oxidized to form cystine, a dimer of two cysteine molecules, connected via a disulfide bridge that are more stable than cysteine.

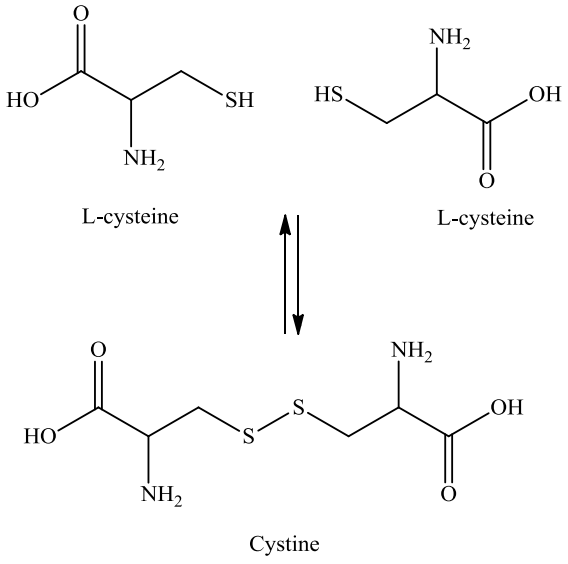

Figure 5.14 Reversible reaction between L-cysteine and cystine

Figure 5.15 shows the presence of Ag NPs at the centre which is surrounded by L-cysteine. The -OH group of hydrolysis products of malathion seems to form

hydrogen bonding with -OH groups of stable cystine. These hydrogen bonding interactions lead to a decrease in the absorbance of L-cys-Ag NPs as a result of aggregation.

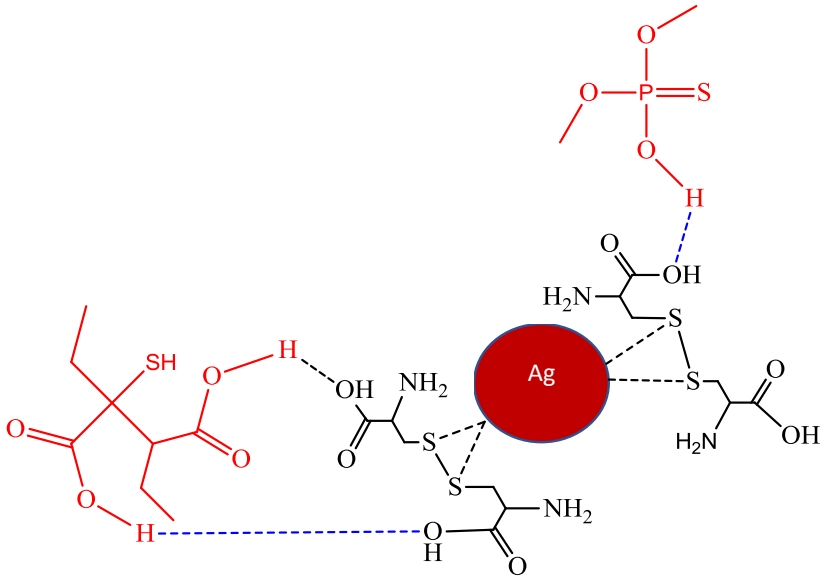

Figure 5.15 Schematic representation for the possible interaction between L-cys-Ag NPs and malathion at acidic pH

CHAPTER VI

CONCLUSION AND FUTURE PROSPECTS

6.1 Conclusion

Green synthesis of Ag NPs using *Parmelia sulcata* extract was successfully done confirmed by absorption peak at 428 nm and 448 nm with and without maintenance of pH as well as a color change. *Parmelia sulcata* has substances that could reduce Ag^{+} to Ag^{0} nanoparticles. L-cysteine modified Ag NPs by forming a shell on the surface through a coordination bond between thiol groups and Ag NPs. Face-centered cubic (FCC) structure with crystal size 7.46 nm was revealed by Powder XRD. SEM results showed that formed Ag NPs were irregular in shape with variable sizes and EDX data confirmed the presence of metallic silver. The L-cys-Ag NPs was reactive to malathion because of the exposed COO^{-} that could detect the positively charged moieties of malathion. NaCl increased the aggregation rate of Ag NPs by bridging the effect of the malathion-Na^{+} complex. With the increase in malathion concentration, the absorbance decreased due to Ag NPs aggregation with the decrease in its color intensity. Thus, L-cys-Ag NPs could be applied as a unique colorimetric sensor for perceiving malathion with different concentrations by changing its color and plasmonic absorbance band of silver nanocolloid.

6.2 Future Prospects

The present research work leaves the following future prospects:

- Optimization of various parameters (effect of temperature, $AgNO_3$ concentration, plant extract concentration etc.) is necessary for a large scale production of the Ag NPs.
- Antibacterial, antifungal, anti-diabetic, anticancer, anti-inflammatory, antiseptic activity of the Ag NPs could also be investigated.
- The toxicity should be tested well for the commercialization of the Ag NPs.
- Besides the study of detection, colorimetric assay should be performed using Ag NPs, other properties and their possible application should be studied.
- Sensing activity of the synthesized Ag NPs regarding different pesticides can be checked.

REFERENCES

1. Barber D. J., Freestone I. C., *Archaeometry*, **1990**, *32*, 33-45.
2. Faraday M., *Phil. Trans. R. Soc. Lond.*, **1857**, *147*, 145-181.
3. Taniguchi N., *Proceeding of the ICPE*, **1974**.
4. Gomaa E. Z., *J. Genetic Eng. Biotechnol.*, **2017**, *15*, 49-57.
5. Sre P. R., Reka M., Poovazhagi R., Kumar M. A., Murugesan K., *Spectrochim. Acta A Mol. Biomol. Spectrosc.*, **2015**, *135*, 1137-1144.
6. Gopinath V., MubarakAli D., Priyadarshini S., Priyadharsshini N. M., Thajuddin N., Velusamy P., *Colloids Surf. B Biointerfaces*, **2012**, *96*, 69-74.
7. Jagtap U. B., Bapat V. A., *Industrial Crops and Products*, **2013**, *46*, 132-137.
8. Panja S., Chaudhuri I., Khanra K., Bhattacharyya N., *Asian Pac. J. Trop. Dis.*, **2016**, *6*, 549-556.
9. Kharissova O. V., Dias H. V. R., Kharisov B. I., Pérez B. O., Pérez V. M. J., *Trends Biotechnol.*, **2013**, *31*, 240-248.
10. Swamy M. K., Sudipta K. M., Jayanta K., Balasubramanya S., *Appl. Nanosci.*, **2015**, *5*, 73-81.
11. Melendez R. G., Moreno K. J., Moggio I., Arias E., Ponce A., Llanera I., MoyaS. E., *Mater. Sci. Forum*, **2010**, *644*, 85-90.
12. Ahmed S., Saifullah, Ahmad M., Swami B. L., Ikram S., *J. Radiat. Res. Appl. Sci.*, **2016**, *9*, 1-7.
13. Phongtongpasuk S., Poadang S., Yongvanich N., *Energy Procedia*, **2016**, *89*, 239-247.
14. Rafique M., Sadaf I., Rafique M. S., Tahir M. B., *Artificial Cells, nanomedicine, and biotechnology*, **2017**, *45*, 1272-1291.
15. Lukman A. I., Gong B., Marjo C. E., Roessner U., Harris A. T., *J. Colloid Interface Sci.*, **2011**, *353*, 433-444.
16. Rajeshkumar S., Bharath L. V., *Chemico-biological Interactions*, **2017**, *273*, 219-227.
17. Singh P., Kim Y. J., Zhang D., Yang D. C., *Trends Biotechnol.*, **2016**, *34*, 588-599.

18. Saxena A., Tripathi R. M., Zafar F., Singh P., *Mater. Lett.*, **2012**, *67*, 91-94.
19. Selvam K., Sudhakar C., Govarthanan M., Thiyagarajan P., Sengottaiyan A., Senthilkumar B., Selvankumar T., *J. Radiat. Res. Appl. Sci.*, **2017**, *10*, 6-12.
20. Khandel P., Yadaw R. K., Soni D. K., Kanwar L., Shahi S. K., *J. Nanostruct. Chem.*, **2018**, *8*, 217-254.
21. Ezealisiji K. M., Noundou X. S., Ukwueze S. E., *Appl. Nanosci.*, **2017**, *7*, 905-911.
22. Velammal S. P., Devi T. A., Amaladhas T. P., *J. Nanostruct. Chem.*, **2016**, *6*, 247-260.
23. Pethakamsetty L., Kothapenta K., Nammi H. R., Ruddaraju L. K., Kollu P., Yoon S. G., Pammi S. V. N., *J. Environ. Sci.*, **2016**, *55*, 157-163.
24. Wang L., Wu Y., Xie J., Wu S., Wu Z., *Mater. Sci. Eng. C*, **2018**, *86*, 1-8.
25. Roopan S. M., Madhumitha G., Rahuman A. A., Kamaraj C., Bharathi A., Surendra T. V., *Industrial Crops and Products*, **2013**, *43*, 631-635.
26. Sadeghi B., Gholamhoseinpoor F., *Spectrochim. Acta A Mol. Biomol. Spectrosc.*, **2015**, *134*, 310-315.
27. Ortega- Arroyo L., Martin- Martinez E. S., Aguilar- Mendez M. A., Cruz- Orea A., Hernandez- Pérez I., Glorieux C., *Starch- Stärke*, **2013**, *65*, 814-821.
28. Tagad C. K., Dugasani S. R., Aiyer R., Park S., Kulkarni A., Sabharwal S., *Sens. Actuators B Chem.*, **2013**, *183*, 144-149.
29. Vanaja M., Rajeshkumar S., Paulkumar K., Gnanajobitha G., Malarkodi C., Annadurai G., *Adv. Appl. Sci. Res.*, **2013**, *4*, 50-55.
30. Ibrahim H. M. M., *J. Radiat. Res. Appl. Sci.*, **2015**, *8*, 265-275.
31. Sastry M., Mayya K. S., Bandyopadhyay K., *Colloids Surf. A Physicochem. Eng. Asp.*, **1997**, *127*, 221-228.
32. Donarski W. J., Dumas D. P., Heitmeyer D. P., Lewis V. E., Raushel F. M., *Biochemistry*, **1989**, *28*, 4650-4655.
33. Chapalamadugu S., Chaudhry G. R., *Crit. Rev. Biotechnol.*, **1992**, *12*, 357-389.

34. Panyala N. R., Peña-Méndez E. M., Havel J., *J. Appl. Biomed.*, **2008**, *6*, 117-129.
35. Drake P. L., Hazelwood K. J., *The Annals of Occupational Hygiene*, **2005**, *49*, 575-585.
36. Kittler S., Greulich C., Diendorf J., Koller M., Epple M., *Chem. Mater.*, **2010**, *22*, 4548-4554.
37. Bai R. G., Sabouni R., Husseini G., *Applications of Nanomaterials*, **2018**, 133-159.
38. Csaki A., Stranik O., Fritzsche W., *Expert. Rev. Mol. Diagn.*, **2018**, *18*, 279-296.
39. Amirjani A., Bagheri M., Heydari M., Hesaraki S., *Nanotechnology*, **2016**, *27*, 375503.
40. Detsri E., Seeharaj P., Sriwong C., *Colloids Surf. A Physicochem. Eng. Asp.*, **2018**, *541*, 36-42.
41. Gao Y., Wu Y., Di J., *Spectrochim. Acta A Mol. Biomol. Spectrosc.*, **2017**, *173*, 207-212.
42. Qin L., Zeng G., Lai C., Huang D., Xu P., Zhang C., Cheng M., Liu X., Liu S., Li B., Yi H., *Coord. Chem. Rev.*, **2018**, *359*, 1-31.
43. Hale Jr M. E., *Smithsonian Contributions to Botany*, **1987**.
44. Manojlović N., Ranković B., Kosanić M., Vasiljević P., Stanojković- T., *Phytomed.*, **2012**, *19*, 1166-1172.
45. Rawtani D., Khatri N., Tyagi S., Pandey G., *J. Environ. Manag.*, **2018**, *206*, 749-762.
46. Li H., Li F., Han C., Cui Z., Xie G., Zhang A., *Sens. Actuators B Chem.*, **2010**, *145*, 194-199.
47. Dubas S. T., Pimpan V., *Mater. Lett.*, **2008**, *62*, 2661-2663.
48. Xiong D., Li H., *Nanotechnology*, **2008**, *19*, 465502.
49. Lisha K. P., Anshup, Pradeep T., *J. Environ. Sci. Health B*, **2009**, *44*, 697-705.
50. Chai F., Wang C., Wang T., Ma Z., Su Z., *Nanotechnology*, **2009**, *21*, 025501.
51. Park Y., Im A., Hong Y. N., Kim C. K., Kim Y. S., *J. Nanosci. Nanotechnol.*, **2011**, *11*, 7570-7578.

52. Zheng J., Zhang H., Qu J., Zhu Q., Chen X., *Anal. Methods*, **2013**, *5*, 917-924.
53. Menon S. K., Modi N. R., Pandya A., Lodha A., *RSC Adv.*, **2013**, *3*, 10623-10627.
54. Vasimalai N., John S. A., *Talanta*, **2013**, *115*, 24-31.
55. D'Souza S. L., Pati R. K., Kailasa S. K., *Anal. Methods*, **2014**, *6*, 9007-9014.
56. Wang X., Yang Y., Dong J., Bei F., Ai S., *Sens. Actuators B Chem.*, **2014**, *204*, 119-124.
57. Li Z., Wang Y., Ni Y., Kokot S., *Sens. Actuators B Chem.*, **2014**, *193*, 205-211.
58. Liu G., Yang X., Li T., Yu H., Du X., She Y., Wang J., Wang S., Jin F., Jin M., Shao H., *Microchim. Acta*, **2015**, *182*, 1983-1989.
59. Kodir A., Imawan C., Permana I. S., Handayani W., *International Seminar on Sensors, Instrumentation, Measurement and Metrology (ISSIMM)*, **2016**, 43-47.
60. Bala R., Dhingra S., Kumar M., Bansal K., Mittal S., Sharma R. K., Wangoo N., *Chem. Eng. J.*, **2016**, *311*, 111-116.
61. Wu S., Li D., Wang J., Zhao Y., Dong S., Wang X., *Sens. Actuator B Chem.*, **2017**, *238*, 427-433.
62. Siangproh W., Somboonsuk T., Chailapakul O., Songsrirote K., *Talanta*, **2017**, *174*, 448-453.
63. Luo Q. J., Li Y. X., Zhang M. Q., Qui P., Deng Y. H., *Chin. Chem. Lett.*, **2017**, *28*, 345-349.
64. Liou P., Nayigiziki F. X., Kong F., Mustapha A., Lin M., *Carbohydr. Polym.*, **2017**, *157*, 643-650.
65. Chen N., Liu H., Zhang Y., Zhou Z., Fan W., Yu G., Shen Z., Wu A., *Sens. Actuators B Chem.*, **2018**, *255*, 3093-3101.
66. Wang Z., Huang Y., Wang D., Sun L., Dong C., Fang L., Zhang Y., Wu A., *Anal. Methods*, **2018**, *10*, 1774-1780.
67. Kang J. Y., Zhang Y. J., Li X., Dong C., Liu H. Y., Miao L. J., Low P. J., Gao Z. X., Hosmane N. S., Wu A. G., *Anal. Methods*, **2018**, *10*, 417-421.

68. Ma S., He J., Guo M., Sun X., Zheng M., Wang Y., *Colloids Surf. A Physicochem. Eng. Asp.*, **2018**, *538*, 343-349.
69. Rana K., Bhamore J. R., Rohit J. V., Park T. J., Kailasa S. K., *New J. Chem.*, **2018**, *42*, 9080-9090.
70. Singhal A., Lind M. L., *Inter. J. Nanomed.*, **2018**, *13*, 25.
71. Abnous K., Danesh N. M., Ramezani M., Alibolandi M., Emrani A. S., Lavaee P., Taghdisi S. M., *Microchim. Acta*, **2018**, *185*, 216.
72. Li D., Wang S., Wang L., Zhang H., Hu J., *Anal. Bioanal.Chem.*, **2019**, *411*, 2645-2652.
73. Ghoto S. A., Khuhawar M. Y., Jahangir T. M., *Anal. Sci.*, **2019**, *18*, 417.
74. Khalkho B. R., Kurrey R., Deb M. K., Shrivas K., Thakur S. S., Pervez S., Jain V. K., *Heliyon*, **2020**, 6, e03423.
75. Mie R., Samsudin M. W., Din L. B., Ahmad A., Ibrahim N., Adnan S. N. A., *Intl. J. Nanomedicine*, **2014**, *9*, 121-127.
76. Mulvaney P., *Langmuir*, **1996**, *12*, 788-800.
77. Kelly K. L., Coronado E., Zhao L. L., Schatz G. C., *J. Physc. Chem. B*, **2003**, *107*, 668-677.
78. Krishnaraj C., Jagan E. C., Rajasekar S., Selvakumar P., Kalaichelvan P. T., Mohan N., *Colloids Surf. B Biointerfaces*, **2010**, *76*, 50-56.
79. Veerasamy R., Xin T. Z., Gunasagaran S., Xiang T. F. W., Yang E. F. C., Jeyakumar N., Dhanaraj S. A., *Journal of Saudi Chemical Society*, **2011**, *15*, 113-120.
80. Jain D., Daima H. K., Kachhwaha S., Kothari S. L., *Dig. J. Nanomater. Biostruct.*, **2009**, *4*, 557-563.V
81. Cruz D., Falé P. L., Mourato A., Vaz P. D., Serralheiro M. L., Lino A. R. L., *Colloids Surf. B Biointerfaces*, **2010**, *81*, 67-73.
82. Gilaki M., *J. Biol. Sci.*, **2010**, *10*, 465-467.
83. Mehmood A., Murtaza G., Bhatti T. M., Kausar R., *Arab. J. Chem.*, **2017**, *10*, 3048-3053.
84. Fayaz A. M., Balaji K., Kalaichelvan P. T., Venkatesan R., *Colloids Surf. B Biointerfaces*, **2009**, *74*, 123-126.
85. Ahmad N., Sharma S., Alam M. K., Singh V. N., Shamsi S. F., Mehta B. R., Fatma A., *Colloids Surf. B Biointerfaces*, **2010**, *81*, 81-86.

86. Davied F., Elix J. A., Samsudin M. W., *Aust. J. Chem*., **1990**, *43*, 1297-1300.
87. Djuhana D., Putra M. H., Imawan C., Fauzia V., Harmoko A., Handayani W., Ardani H., *AIP Conference Proceedings*, **2016**, *1729*, 020023.
88. Chen S. F., Zhang H., *Adv. Nat. Sci. Nanosci. Nanotechnol.*, **2012**, *3*, 035006.
89. Faria I. R., Palumbo A. J., Fojut T. L., *Dept. Environ. Toxicology*, **2010**.
90. Steiner T., *Angew. Chem. Int. Ed*., **2002**, *41*, 48-76.
91. Bhumkar D. R., Joshi H. M., Sastry M., Pokharkar V. B., *Pharmaceut. Res*., **2007**, *24*, 1415-1426.

ANNEX

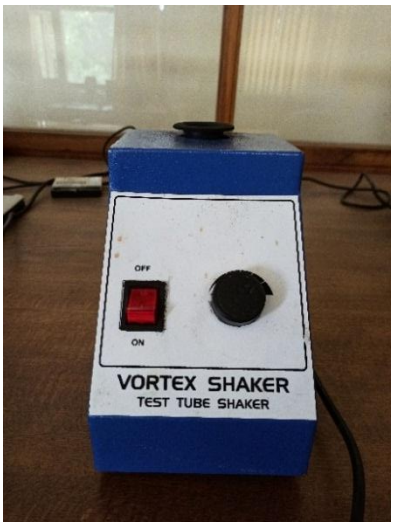

Pictures of materials and instruments